Modeling and Analysis of a Tensegrity-Based Vibratory Platform Driven by Piezoelectric Actuators Using IronCAD

Wen-Hsiang Hsieh*, Samudra Prasetyo*, Chen-Ji Pan

Department of Automation Engineering, National Formosa University, Yunlin, Taiwan, ROC

Received 25 April 2025; received in revised form 18 November 2025; accepted 20 November 2025

DOI: https://doi.org/10.46604/peti.2025.15076

Abstract

This study aims to perform a simulation study of a tensegrity-based vibratory platform driven by piezoelectrical actuators using IronCAD software. The platform can advance parts in a specified rotational displacement. The platform's structure is presented first. Then, the proposed platform's solid model is established using IronCAD software. Moreover, piezoelectric actuators are modeled in Multiphysics for IronCAD by specifying the piezoelectric material properties. Various inputs to the platform are simulated and investigated. The simulation results demonstrate the effectiveness of IronCAD for modeling and analyzing the proposed design.

Keywords: tensegrity, vibratory platform, Piezoelectric Actuator, IronCAD, conveyor

1. Introduction

A feeder, or conveyor, is a mechanical system intended to continuously or intermittently move items along a predetermined direction. Feeder systems are commonly used in diverse production processes for cost-effective and efficient bulk material handling. They are crucial in various industries, including electronics, food, pharmaceuticals, machinery, and chemicals, as vital tools in contemporary automation [1].

Feeder systems are adaptable and can be employed for tasks such as sorting, orienting, and separating materials, serving as commonly used automated feeding mechanisms. In contrast to traditional continuous belt conveyors, vibratory feeders are characterized by their periodic back-and-forth vibrations, which enable parts to slide along the trough and move forward. Vibratory conveyors have multiple benefits, including a compact design, the ability to align parts, and their effectiveness in managing high-temperature or small-quantity materials [2].

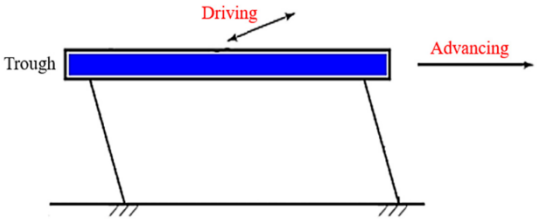

Fig. 1 Inline vibratory platform [3]

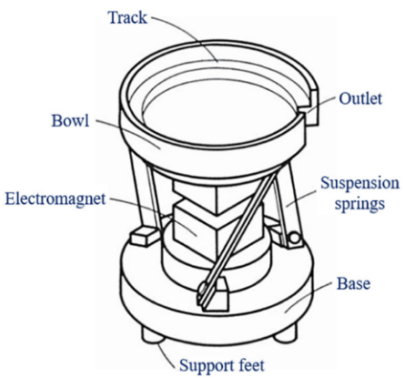

Fig. 2 Vibratory bowl conveyor [4]

* Corresponding author. E-mail address: allen@nfu.edu.tw; samudra2702@gmail.com

Vibratory conveyors generally consist of actuators that create vibrations, troughs (or tubes) that carry objects or bulk materials, and springs (elastic components) that support the troughs elastically. The two main types of vibratory feeders, which differ based on the movement path of the material or the design of the trough, are linear vibratory conveyors and vibratory bowl feeders, as shown in Fig. 1 [3] and Fig. 2 [4], respectively. The actuator-generated vibrations help move materials along the trough. Despite their effectiveness, vibratory feeders have several drawbacks, such as excessive noise, large designs, slow feeding speeds, and vulnerability to damage to parts. Furthermore, fatigue caused by vibrations can shorten their operational lifespan. In light of these challenges, multiple initiatives have been made to improve their performance and durability.

As shown in Fig. 3, Tensegrity structures offer numerous advantages that enhance structural performance and material efficiency. A significant benefit is their capability to distribute loads uniformly across the entire structure, thereby removing critical weakness points often found in conventional continuous designs. This characteristic improves durability and allows tensegrity systems to absorb shocks and vibrations effectively, making them ideal for uses such as earthquake-resistant buildings and bridges [5]. Furthermore, the lightweight quality of tensegrity structures results in considerable material savings while preserving structural integrity, opening doors for innovative architectural designs and efficient building methods [6]. Their built-in flexibility also facilitates quick load transfer, which is crucial in dynamic settings, emphasizing their adaptability in contemporary engineering applications [7].

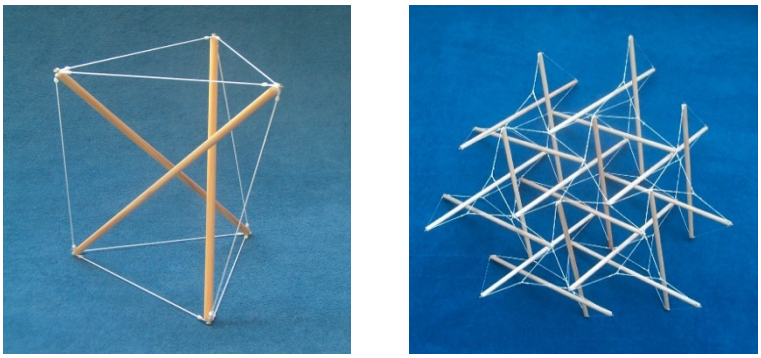

Fig. 3 Tensegrity structure [8]

Tensegrity is a structural design principle that combines isolated compression elements with a continuous network of tensile components. Its history dates back to the mid-20th century, gaining attention from architects and engineers focused on material efficiency. The term "tensegrity" was coined by architect Buckminster Fuller in the 1960s, inspired by Kenneth Snelson's 1948 "X-Piece," the first known tensegrity structure. Fuller proposed a tensegrity-icosahedron in 1951, demonstrating stability and material savings [9-10]. Over the following decades, tensegrity gained popularity in art and engineering [11], with applications in lightweight constructions and robotics. Research by academics like Pellegrino and Calladine further established its engineering relevance [12]. As interest in sustainable design grows, tensegrity's principles are increasingly recognized for reducing material waste and enhancing architectural resilience.

Discovered by Pierre and Jacques Curie in 1880, piezoelectricity is the phenomenon where certain materials generate an electric charge under mechanical stress. The term "piezoelectricity" is derived from the Greek word "piezein," meaning "to press," and refers to the ability of materials such as crystals, ceramics, and biological substances to produce an electric potential when deformed [3, 13]. This effect is reversible; applying an electric field to a piezoelectric material can induce mechanical deformation. The underlying mechanism displaces positive and negative charges within the material's crystal lattice, leading to net polarization under stress [14].

Although vibratory platforms, tensegrity structures, and piezoelectric actuators have each been studied independently, their integration into a single system has received limited attention in the published literature. Moreover, the use of IronCAD as a modeling and simulation environment for such hybrid configurations has not been widely explored. To address this gap, the present study employs IronCAD to investigate the motion characteristics of a tensegrity-based vibratory platform actuated by piezoelectric elements.

This study aims to simulate the advanced motion of a tensegrity-based vibratory platform using piezoelectric actuators in IronCAD. Tensegrity structures, composed of rigid elements and tensioned cables, offer stability and lightweight design, with applications in fields like robotics. Vibratory platforms generate vibrations for material transport tasks such as classification and separation. This simulation explores how piezoelectric actuators enhance the platform's motion and demonstrates the effectiveness of IronCAD for modeling such systems.

2. Proposed Platform

This study aims to simulate the advanced motion of the platform, as shown in Fig. 4. To obtain the anticipated outcomes, it is crucial to finalize the design of the tensegrity-based vibratory platform along with the integration of the piezoelectric actuators. IronCAD software has been selected due to its intuitive interface, which not only simplifies the process of finite element analysis but also allows for precise simulation of piezoelectric materials. This combination of features will enable a thorough exploration of the platform's mechanical behavior and the effectiveness of the actuators in real-world applications.

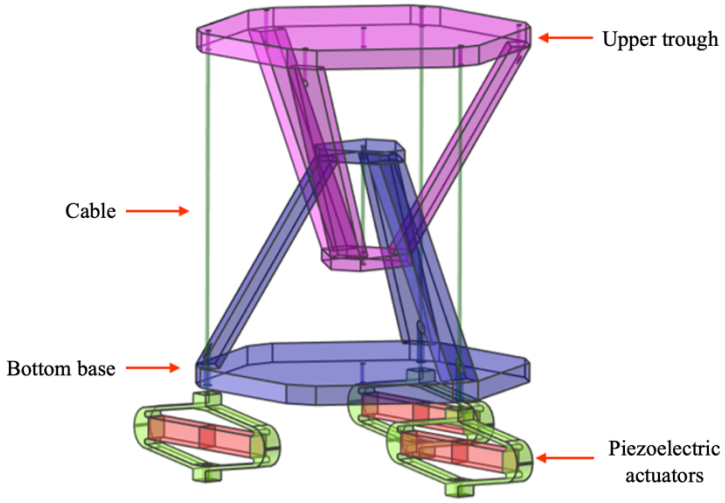

Fig. 4 Tensegrity-based vibratory platform

The platform consists of four ropes, an upper trough, a bottom base, and three piezoelectric actuators. Its tensegrity structure allows it to maintain a static equilibrium position while also facilitating movement. By manipulating the cables through tension and compression in an oscillating manner, the upper trough vibrates, producing a conveying motion in a designated direction on the platform. This design is well-suited for the precise transport of small parts and high-speed movement.

The materials employed in constructing the proposed platform are acrylonitrile butadiene styrene (ABS) and nylon. The ABS is assigned to the upper trough and bottom base, represented in purple and blue, respectively, while the nylon is assigned to the cables, represented in green. The detailed material properties for ABS and nylon are listed in Table 1.

Table 1 Property of ABS and nylon

Material Type	Property	Value	Unit
ABS	Young's modulus	2000	N/mm^2
	Poisson's ratio	0.394	-
	Mass density	1.02×10^{-6}	kg/mm^3
Nylon	Young's modulus	1000	N/mm^2
	Poisson's ratio	0.3	-
	Mass density	1.15×10^{-6}	kg/mm^3

The piezoelectric actuator is the main component responsible for generating tension on the cable. When a voltage is applied to the actuator, it exerts a downward force on the cable, generating tension. Once the actuator is deactivated, the cable returns to its original position. This oscillatory motion of the actuator produces a net forward displacement of the part by ensuring that the forward acceleration is greater than the backward acceleration; the difference in acceleration results in a sliding effect that facilitates forward motion.

3. Piezoelectric Material and Actuator

Piezoelectric materials, including quartz and lead zirconate titanate (PZT), have found extensive applications in modern technology, ranging from sensors and actuators to energy harvesting devices, underscoring their significance in various fields such as electronics, robotics, and biomedical engineering. Their unique ability to convert mechanical stress into electrical energy makes them invaluable for innovations in these areas, enhancing system efficiency and performance [15].

In piezoelectric materials, the mechanical and electrical fields are coupled such that an applied stress produces an electric displacement and an applied electric field produces a strain. This electromechanical behavior can be described by the linear constitutive relations. In the strain-charge form, the strain tensor is expressed as [16]

$$\varepsilon_{ij} = s^{E}_{ijkl}\sigma_{kl} + d_{kij}E_{k} \tag{1}$$

This tensor expression can be further simplified by adopting the contracted Voigt notation, which reduces the fourth-order tensors into matrix form. The representation of a compact matrix form that explicitly incorporates the coupling between mechanical and electrical variables which can be computed as

$$S = \underbrace{s^{E}}_{6\times6} T + \underbrace{d^{T}}_{6\times3} E \tag{2}$$

where compliance matrix s^E defines the elastic behavior of piezoelectric materials under a constant electric field. Due to crystal symmetry, many components are identical or zero, reducing the matrix to the simplified form. In this representation, $s^E_{66} = 2(s^E_{11} - s^E_{12})$, reflecting the material's isotropy in the transverse plane which can be represented as

$$s^{E} = \begin{bmatrix} s^{E}_{11} & s^{E}_{12} & s^{E}_{13} & 0 & 0 & 0 \\ s^{E}_{21} & s^{E}_{22} & s^{E}_{23} & 0 & 0 & 0 \\ s^{E}_{31} & s^{E}_{32} & s^{E}_{33} & 0 & 0 & 0 \\ 0 & 0 & 0 & s^{E}_{44} & 0 & 0 \\ 0 & 0 & 0 & 0 & s^{E}_{55} & 0 \\ 0 & 0 & 0 & 0 & 0 & s^{E}_{66} \end{bmatrix} \tag{3}$$

where piezoelectric coupling matrix d^T characterizes the interaction between the mechanical and electrical fields by relating the applied electric field to the induced strain. These coefficients determine the strength and directionality of the electromechanical coupling in PZT materials which is defined as

$$d^{T} = \begin{bmatrix} 0 & 0 & d_{31} \\ 0 & 0 & d_{32} \\ 0 & 0 & d_{33} \\ 0 & d_{24} & 0 \\ d_{15} & 0 & 0 \\ 0 & 0 & 0 \end{bmatrix} \tag{4}$$

When the compliance matrix and piezoelectric coupling matrix are combined, the strain–charge relation can be expressed in its expanded form as [17]

$$\begin{bmatrix} S_1 \\ S_2 \\ S_3 \\ S_4 \\ S_5 \\ S_6 \end{bmatrix} = \begin{bmatrix} s_{11}^E & s_{12}^E & s_{13}^E & 0 & 0 & 0 \\ s_{21}^E & s_{22}^E & s_{23}^E & 0 & 0 & 0 \\ s_{31}^E & s_{32}^E & s_{33}^E & 0 & 0 & 0 \\ 0 & 0 & 0 & s_{44}^E & 0 & 0 \\ 0 & 0 & 0 & 0 & s_{55}^E & 0 \\ 0 & 0 & 0 & 0 & 0 & s_{66}^E = 2(s_{11}^E - s_{12}^E) \end{bmatrix} \begin{bmatrix} T_1 \\ T_2 \\ T_3 \\ T_4 \\ T_5 \\ T_6 \end{bmatrix} + \begin{bmatrix} 0 & 0 & d_{31} \\ 0 & 0 & d_{32} \\ 0 & 0 & d_{33} \\ 0 & d_{24} & 0 \\ d_{15} & 0 & 0 \\ 0 & 0 & 0 \end{bmatrix} \begin{bmatrix} E_1 \\ E_2 \\ E_3 \end{bmatrix} \tag{5}$$

Piezoelectric actuators convert electrical energy into mechanical motion using the inverse piezoelectric effect and are found in aerospace, precision machining, microscopy, and micro-manipulation. Utilizing materials like PZT, these actuators enable high-resolution positioning at the nanometer scale. The strain generated from the piezoelectric actuator is too small; therefore, using an amplifying piezoelectric actuator can produce greater displacement from the piezoelectric material. Their advantages include rapid response, compact size, low power consumption [18], and high displacement resolution, making them suitable for optical scanning, fluid control, and vibration isolation. Additionally, piezoelectric actuators suffer from inherent nonlinear characteristics such as vibration and hysteresis. However, these nonlinear characteristics of vibrations and hysteresis will be utilized for applications in vibration systems for this platform [19].

The piezoelectric actuator model was designed using IronCAD software and integrated into the Tensegrity-Based Vibratory Platform, which employs three actuators in its final design. Finite Element Analysis (FEA) is utilized to simulate the advanced motion of the platform. The simulation setup involves defining various parameters in IronCAD, including analysis type, model type, materials, constraints, and mesh. IronCAD is particularly advantageous due to its compatibility with piezoelectric material properties, enabling accurate simulation of the motion of actuators and, consequently, the advanced motion of the platform. The results are analyzed and presented within IronCAD Multiphysics.

4. Modeling

The process will begin with modeling the piezoelectric actuator in IronCAD, based on the design from APA150M. This actuator is an amplifying piezoelectric device manufactured by Cedrat Technologies. The design of the real-life model is illustrated in Fig. 5, while Fig. 6 displays the actuator model created using IronCAD.

This research employs IronCAD to model and simulate tensegrity-based vibratory platforms along with piezoelectric actuators, utilizing its advanced design and finite element analysis capabilities. The methodology begins with modeling the tensegrity structure, followed by simulating the piezoelectric actuators. This approach allows for an evaluation of their impact on the motion of the platform under various conditions. A flowchart summarizing the methodology is included in Fig. 7 to outline the research process clearly.

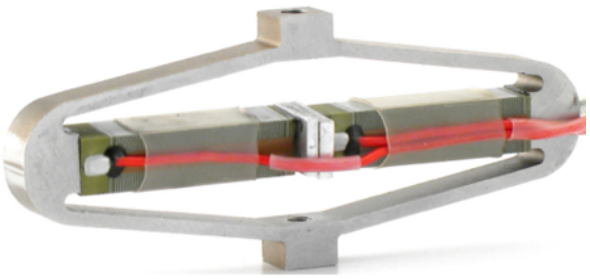

Fig. 5 APA150M piezoelectric actuator

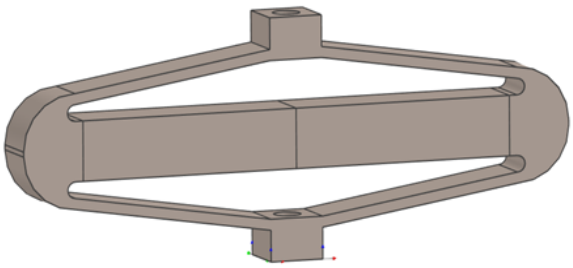

Fig. 6 APA150M piezoelectric actuator designed in IronCAD

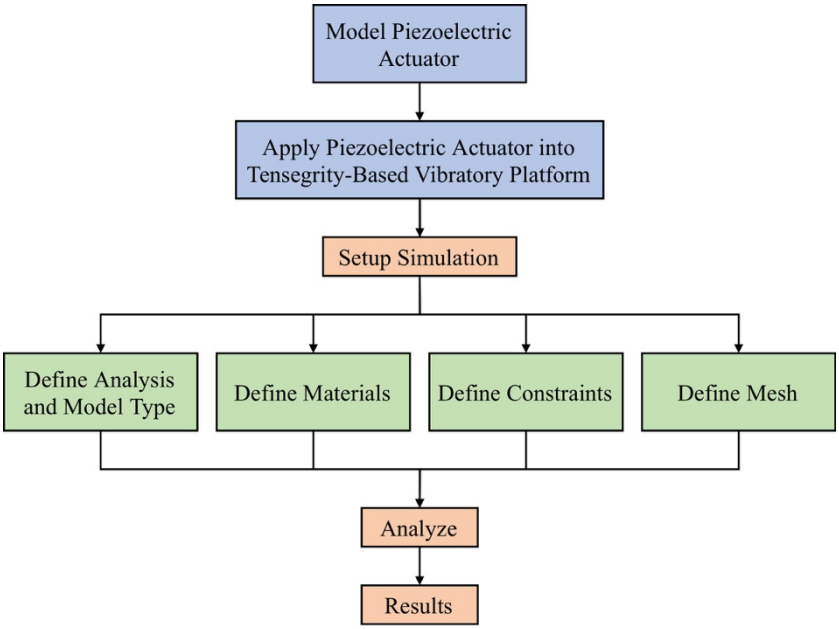

Fig. 7 Modeling and simulation flowchart

The actuator geometry was modeled in IronCAD by constructing a base block and subsequently defining the piezoelectric component through additional extrusion features. The cross-section and placement of these elements were adjusted to match the required design specifications. The resulting geometry is illustrated in Fig. 8. The geometry properties of piezoelectric actuator are listed in Table 2.

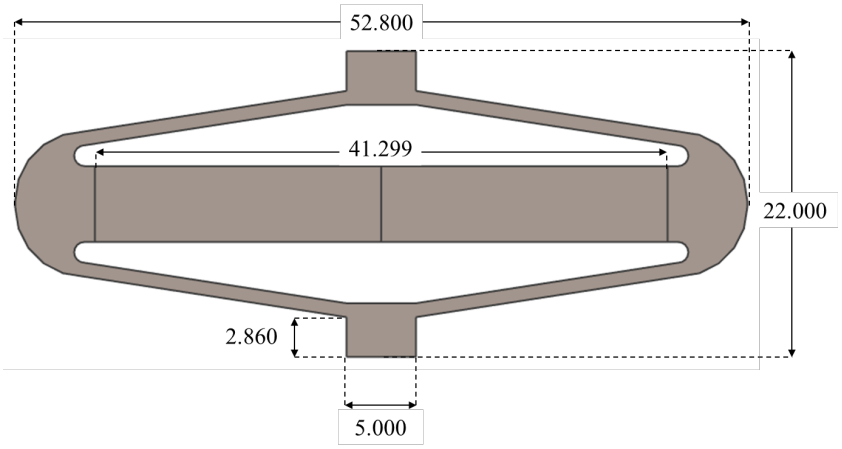

Fig. 8 Geometry of piezoelectric actuator

Table 2 Geometry properties of piezoelectric actuator

Parameter	Value (mm)
Overall length	52.800
Overall height	22.000
Overall thickness	5.000
Piezoelectric material length	41.299
Base width	5.000
Base thickness	2.860

After creating the piezoelectric actuators, they are assembled onto a tensegrity-based vibratory platform. Three different actuators are attached to the ropes at the base area. The assembled components are illustrated in Fig. 9. This configuration ensures that the actuators work together to produce the desired oscillatory motion for the platform. The bottoms of the piezoelectric actuators are fixed in place, allowing displacement to occur only at the upper side of the actuators.

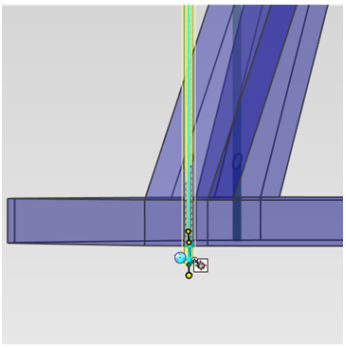

(a) Create tolerance for cable-actuator connection

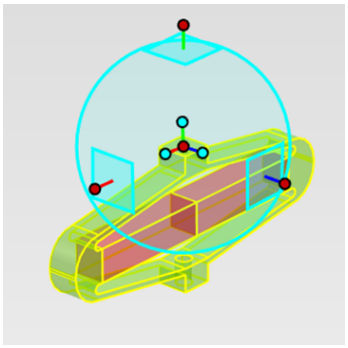

(b) Moving actuator using triBall

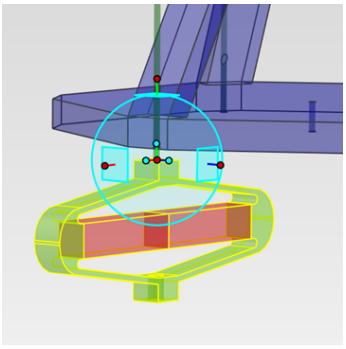

(c) Connect the cable and the actuator

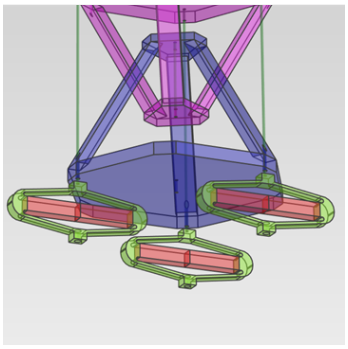

(d) Connecting all actuators to cables

Fig. 9 Assembling the piezoelectric actuator on the platform

IronCAD is renowned for its user-friendly interface and rapid modeling capabilities. One of its standout features, the TriBall tool, greatly simplifies the assembly of parts with minimal effort. The TriBall function allows users to designate the point to which a part should be moved, as well as to duplicate and copy parts simply by clicking on the tool. Furthermore, it facilitates movement along a specific axis and offers options for rotational movement around the chosen axis.

5. Simulation

The piezoelectric actuator and the proposed platform have a complex geometry that includes piezoelectric material. Therefore, it is essential to conduct a FEA to verify both the deformation and the direction of motion of the proposed platform and the piezoelectric actuator. This analysis will focus on the advanced motion of the proposed platform when the piezoelectric actuator is activated with voltage, which induces strain or deformation in the platform. The analysis uses the Multiphysics module in IronCAD, a simulation tool integrated into the IronCAD software.

5.1. Piezoelectric Actuator Simulation

The simulation of the piezoelectric actuator was conducted in IronCAD Multiphysics using a three-dimensional dynamic/transient analysis. The electro-physics module was activated to account for the dielectric behavior of piezoelectric materials, and the dielectric property was included in the model definition. Additional materials required for the simulation were defined through the material editor, and all parameters were specified in the Metric-MKS unit system (millimeters, Newtons, kilograms, seconds).

In the material definition stage, two materials were specified which are aluminum and the piezoelectric ceramic PZT-5A. Aluminum 1050 (GB), available in the IronCAD database, was selected directly with its predefined properties. For the piezoelectric actuator, a non-linear anisotropic material with electro-mechanical coupling was defined, and the electrical properties of PZT-5A were refined by assigning the dielectric constant and piezoelectric charge parameters, as listed in Tables

3, while the mechanical properties of Aluminum and PZT-5A are summarized in Table 4. The piezo-strain matrix was employed in this simulation to represent the inverse piezoelectric effect. The material layout of the piezoelectric actuator in shown in Fig. 10, where red represent PZT-5A and blue represent Aluminum 1050 (GB).

Table 3 Electrical property of PZT-5A

Property	Value	Unit
Dielectric constant	1800	V/mm
Piezoelectric charge (d_{31})	-0.00019	μC/N
Piezoelectric charge (d_{33})	0.00039	μC/N

Table 4 Mechanical property of Aluminum and PZT-5A

Material type	Property	Value	Unit
Aluminum	Young's modulus	69000	N/mm²
	Poisson's ratio	0.33	-
	Mass density	2.7×10^{-6}	kg/mm³
PZT-5A	Young's modulus	66000	N/mm²
	Poisson's ratio	0.34	-
	Mass density	7.95×10^{-6}	kg/mm³

The definition of piezoelectric material behavior in IronCAD required assigning voltage gradients and coupling coefficients along the principal axes. Voltage Gradient 1 was associated with the X-axis, Voltage Gradient 2 with the Y-axis, and Voltage Gradient 3 with the Z-axis. The corresponding coefficients were entered according to the direction of the applied voltage. The principal material axes were designated as S11, S22, and S33. Since the simulation employed the mm-kg-s unit system, the coefficients obtained from the datasheet were adjusted by an appropriate scaling factor to ensure consistency. In this model, d31 was represented along S11 and S22, while d33 corresponded to S33.

The constraints used in this simulation include fixed points and two applied voltages. The fixed points are located at the bottom of the piezoelectric actuator, while the voltages are applied to each end of the piezoelectric material. A voltage of 150V is applied at one end, while the other end is grounded at 0V. The voltage is applied to the face of the piezoelectric material. After all the constraints are applied, the geometry is meshed using the default settings implemented in IronCAD. The mesh of the geometry can be seen in Fig. 11.

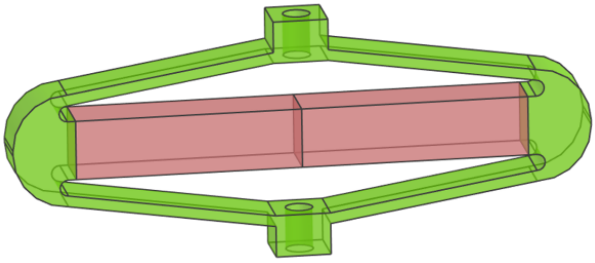

Fig. 10 Material layout of piezoelectric actuator

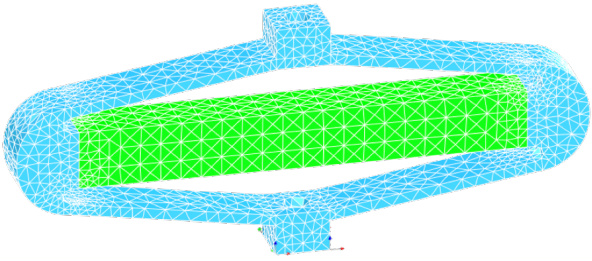

Fig. 11 Mesh of piezoelectric actuator

After analyzing the simulation results, the Animate Scale effectively illustrates the deformation of the actuator caused by the piezoelectric materials. FEA reveals the movement of the piezoelectric actuator, which experiences tension that results in a downward displacement. The maximum deformation recorded for the model was 0.107 mm. The scale utilizes color coding to indicate the extent of deformation, with red representing the highest levels of deformation and blue indicating the lowest. In Fig. 12, the left side displays the expected motion of the actuator, while the right side shows the simulated motion. The red arrow indicates the direction of motion, while the dotted lines show the equilibrium position.

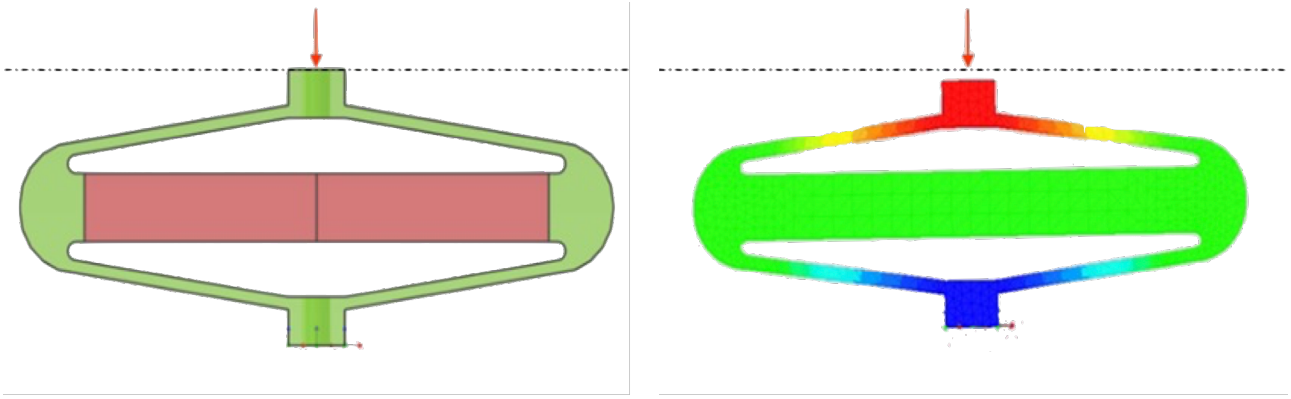

Fig. 12 Expected motion direction and actual motion direction

5.2. Proposed Platform Simulations

In the simulation of the proposed platform, the advanced motion generated by the actuators is analyzed to determine whether the platform can be utilized as a tensegrity-based vibratory system. Several test cases are conducted to evaluate the accuracy and reliability of the motion response, with the platform subjected to displacements of 150° counterclockwise, 60° counterclockwise, and 60° clockwise. These motions are induced through the activation of one, two, and three actuators, respectively.

The simulation setup for the proposed platform follows the same principles as the piezoelectric actuator simulation. A fixed-point constraint is applied at the bottom base to stabilize the model. The voltage supplied to the actuator is defined as a sinewave signal, replicating the operational response of the piezoelectric actuator. Since IronCAD does not natively generate the required waveform, a CSV file was created to define the custom signal and imported into the software by configuring the time dependency entry to precise-linear mode. Once imported, the waveform is displayed as a three-cycle sine function, with each cycle occurring over one second. The maximum factor corresponds to 1, while the minimum corresponds to 0.1333, simulating the operating voltage range of 150 V and −20 V, respectively. The sinewave signal is illustrated in Fig. 13.

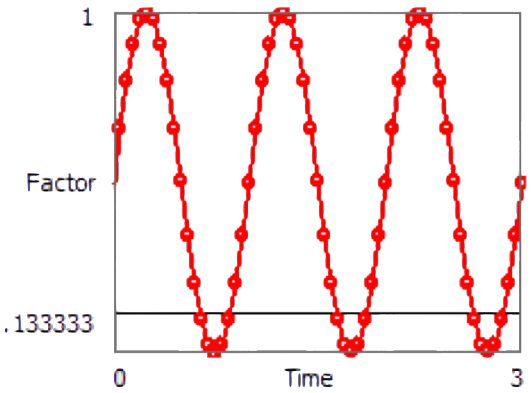

Fig. 13 Sinewave signal of voltage applied to piezoelectric actuator

After conducting the FEA simulation in IronCAD, the result of one piezoelectric actuator, using the full range voltage of 150 V to -20 V, on the platform is evaluated through dynamic simulation. The proposed platform moves towards 150° counterclockwise and the general direction displacement can be seen in Fig. 14. Two reference nodes on the platform are selected to characterize the displacement response: node 211, located on the actuator side of the platform, and node 222, positioned on the opposite side. The displacement along the z-axis is examined to assess the deformation behavior. The displacement along the z-axis indicates that node 211 reaches a peak of -0.09295 mm and 0.01240 mm, while node 222 records -0.00787 mm and 0.05896 mm. The corresponding displacement responses are presented in Fig. 15.

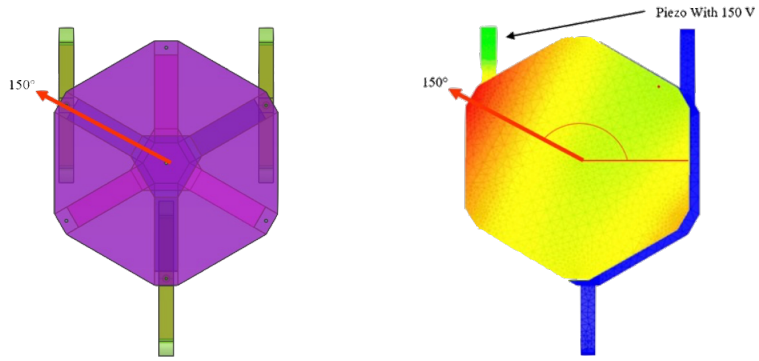

Fig. 14 Expected motion and actual motion direction using one actuator

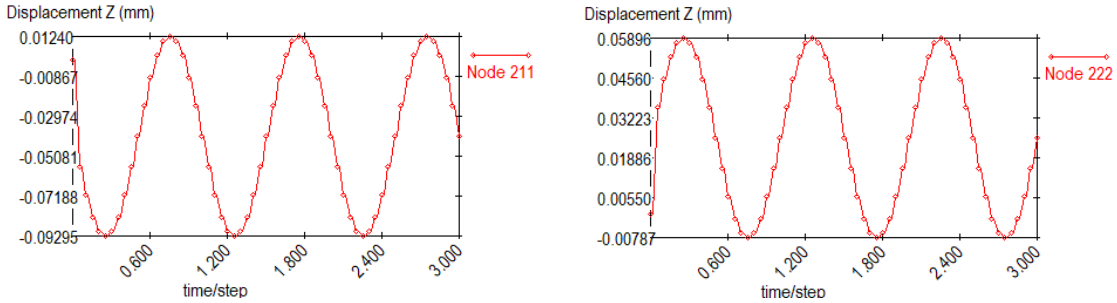

(a) Displacement Z of node 211 (b) Displacement Z of node 222

Fig. 15 Displacement Z of the platform using one actuator

The response of the platform with two piezoelectric actuators activated is also examined. In this case, one actuator is driven with a full voltage range of 150 V to -20 V, while the second actuator is supplied with a reduced range of 75 V to -10 V. The proposed platform moves towards 60° counterclockwise and the general direction displacement can be seen in Fig. 16. Two reference nodes on the platform are selected for analysis: node 214, located at the edge of the platform at 60° counterclockwise, and node 219, positioned on the opposite side. The displacement along the z-axis indicates that node 214 reaches a peak of -0.08087 mm and 0.01079 mm, while node 219 records -0.00483 mm and 0.05896 mm. The corresponding displacement results are illustrated in Fig. 17.

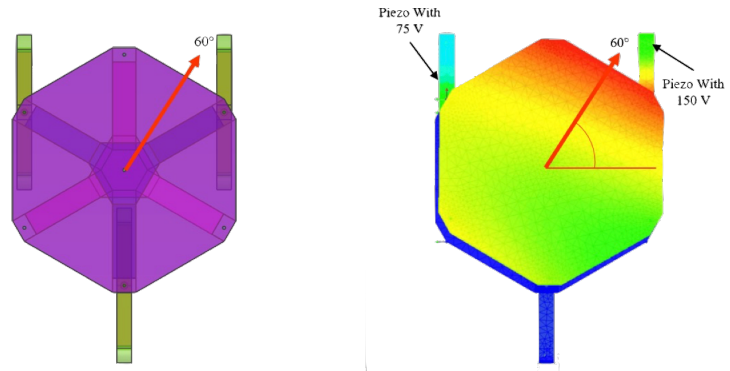

Fig. 16 Expected motion and actual motion direction using two actuators

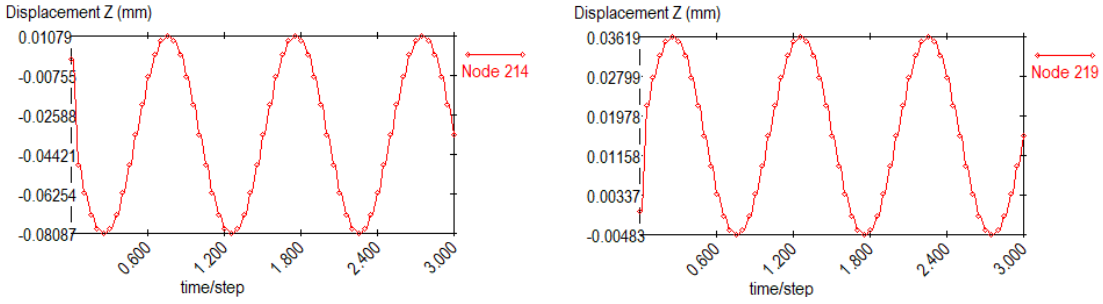

(a) Displacement Z of node 219 (b) Displacement Z of node 214

Fig. 17 Displacement Z of the platform using two actuators

The platform response under the activation of three piezoelectric actuators is further analyzed. The proposed platform moves towards 60° clockwise and the general direction displacement can be seen in Fig. 18. In this case, the first actuator is supplied with a voltage range of 150 V to -20 V, the second actuator operates between 100 V and -13.33 V, and the third actuator is driven from 50 V to -6.67 V. To evaluate the resulting motion, two reference nodes on the platform are selected: node 217, positioned at 60° clockwise, and another node located on the opposite side of the platform. The displacement along the z-axis indicates that node 217 reaches a peak of -0.07187 mm and 0.00959 mm, while node 220 records -0.001092 mm and 0.008171 mm. The corresponding displacement responses are presented in Fig. 19.

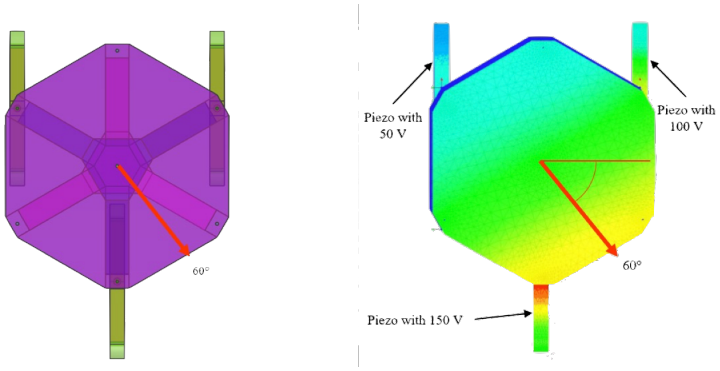

Fig. 18 Expected motion and actual motion direction using three actuators

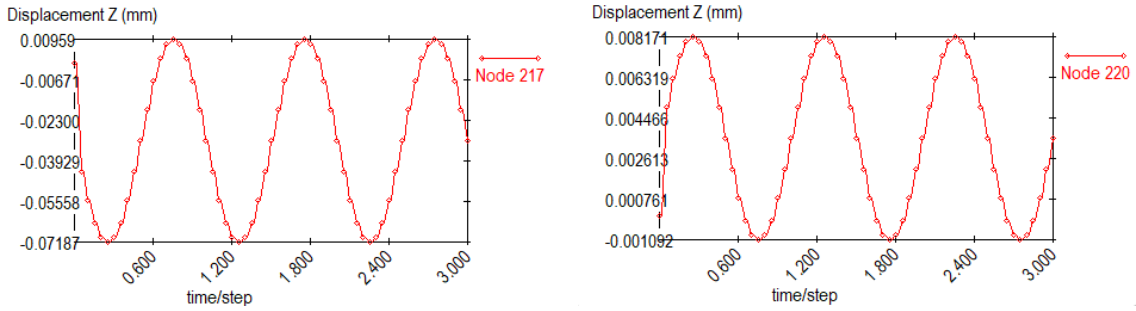

(a) Displacement Z of node 217 (b) Displacement Z of node 220

Fig. 19 Displacement Z of the platform using three actuators

The simulation results demonstrate a linear relationship between the applied voltage and the resulting displacement of the platform. This occurs because the strain in piezoelectric materials is directly proportional to the applied electric field, leading to a corresponding linear displacement response. The outcome confirms that piezoelectric actuation can effectively generate controlled motion, indicating the feasibility of employing the proposed platform as a tensegrity-based vibratory system.

Although the model successfully captures the piezoelectric behavior, it represents an idealized condition intended to isolate the fundamental response of the tensegrity platform. Effects such as material damping, cable slack, and actuator hysteresis were intentionally excluded to focus on the baseline behavior of the structure. Incorporating these nonlinear and dissipative factors in subsequent simulations, along with experimental validation, would provide a more comprehensive understanding of the platform's real-world dynamic performance

6. Conclusions

In this study, FEA was conducted to evaluate the advanced motion of a tensegrity-based vibratory platform and to assess the effectiveness of IronCAD for simulation purposes. The study focused on the interaction between the piezoelectric actuator and the platform, specifically examining how the applied forces influenced platform displacement. Based on the findings, the principal conclusions are as follows.

(1) Based on FEA simulation results, the advanced motion of the tensegrity-based vibratory platform meets the expected motion direction.

(2) IronCAD proved effective for this study because it integrates modeling, automated meshing, and finite element analysis within a single environment. This streamlined workflow reduced setup complexity and allowed direct simulation of piezoelectric material behavior with minimal configuration.

(3) The FEA simulation confirmed that the platform can advance in controlled rotational directions, as demonstrated by test cases at 150° anticlockwise, 60° anticlockwise, and 60° clockwise. In these cases, node displacements ranged from about -0.093 mm to +0.059 mm with one actuator, -0.081 mm to +0.059 mm with two actuators, and -0.072 mm to +0.008 mm with three actuators, indicating consistent directional motion across different actuator configurations

(4) The displacements were directly influenced by the applied piezo actuator forces and were consistent with the expected motion direction. The results further showed a linear relationship between the applied voltage and the resulting displacement for the three actuator cases.

(5) IronCAD is effective for simulating piezoelectric actuators with tensegrity structures because it can directly incorporate piezoelectric material properties, perform coupled electro-mechanical FEA, and handle complex geometries with straightforward modeling tools.

While the findings are promising, the present simulations are limited to idealized conditions in IronCAD. Effects such as damping, nonlinear hysteresis of piezoelectric actuators, and experimental validation were not considered in this work. Future studies should address these aspects to further validate the model and extend its applicability to real-world vibratory conveyor systems

Acknowledgments

The financial support from the National Science Council project (Grant No. MOST 111-2221-E-150-022) is highly appreciated.

Conflicts of Interest

The authors declare no conflict of interest.

References

[1] W. H. Hsieh, C. J. Pan, and Y. C. Hsieh, “Finite Element Analysis of a Novel Tensegrity-Based Vibratory Platform,” International Journal of Engineering and Technology Innovation, vol. 14, no. 1, pp. 58-66, 2024.

[2] C. A. Krülle, A. Götzendorfer, R. Grochowski, I. Rehberg, M. Rouijaa, and P. Walzel, “Granular Flow and Pattern Formation on a Vibratory Conveyor,” Proceedings of Traffic and Granular Flow’05, Berlin, Heidelberg: Springer, pp. 111-128, 2007.

[3] W. H. Hsieh and N. N. Shih, “On an Inline Conveyor Resonantly Driven by Piezoelectric Actuators,” Journal of Vibroengineering, vol. 16, no. 5, pp. 2164-2170, 2014.

[4] D. R. Berkowitz and J. F. Canny, “Designing Parts Feeders Using Dynamic Simulation,” Proceedings of IEEE International Conference on Robotics and Automation, IEEE Press, vol. 2, pp. 1127-1132, 1996.

[5] R. Al Azem, W. Elleithy, T. L. Lau, and M. P. Anwar, “Parametric Study of Tensegrity Structures Under Seismic Loading,” Proceedings of E3S Web of Conferences, EDP Sciences, vol. 347, article no. 03016, 2022.

[6] Y. D. Bansod, D. Nandanwar, and J. Burša, “Overview of Tensegrity-I: Basic Structures,” Engineering Mechanics, vol. 21, pp. 355-367, 2014.

[7] F. Fraternali and F. Santos, “Mechanical Modeling of Superelastic Tensegrity Braces for Earthquake-Proof Structures,” Extreme Mechanics Letters, vol. 33, article no. 100578, 2019.

[8] M. Pars, “Tensegrity,” http://www.tensegriteit.nl/e-simple.html, accessed in 2024.

[9] T. Laila, A. Arruda, J. Barbosa, and E. Moura, “The Constructive Advantages of Buckminster Fuller’s Geodesic Domes and Their Relationship to the Built Environment Ergonomics,” Proceedings of International Conference on Applied Human Factors and Ergonomics, Springer, Cham, vol. 588, pp. 357-368, 2018.

[10] K. Snelson, “The Art of Tensegrity,” International Journal of Space Structures, vol. 27, no. 2-3, pp. 71-80, 2012.

[11] O. Vilnay, L. Chernin, and M. Vilnay, Tensegrity Structures Design Methods, 1st ed., Florida: CRC Press, 2023.
[12] H. R. Drew and S. Pellegrino, New Approaches to Structural Mechanics, Shells and Biological Structures, 1st ed., Dordrecht: Springer, 2002.
[13] Y. Meng, G. Chen, and M. Huang, "Piezoelectric Materials: Properties, Advancements, and Design Strategies for High-Temperature Applications," Nanomaterials, vol. 12, no. 7, article no. 1171, 2022.
[14] Z. Yang, W. Peng, W. Li, S. Su, G. Lin, and J. Chen, "Using a Multi-Layer Graphene-Based Emitter to Improve the Performance of a Concentrated Solar Thermionic Converter," Journal of Applied Physics, vol. 124, no. 15, article no. 154501, 2018.
[15] L. Csoka, I. C. Hoeger, O. J. Rojas, I. Peszlen, J. J. Pawlak, and P. N. Peralta, "Piezoelectric Effect of Cellulose Nanocrystals Thin Films," ACS Macro Letters, vol. 1, no. 7, pp. 867-870, 2012.
[16] S. Lu, G. Lin, Y. Ma, and J. Su, "Static Analysis of Layered Piezoelectric Materials Using the Hamiltonian-Based Derivation Modified SBFEM," Construction and Building Materials, vol. 445, article no. 137732, 2024.
[17] "The Behavior Laws of Piezoelectricity," https://onscale.com/piezoelectricity/the-behavior-laws-of-piezoelectricity/, accessed in 2024.
[18] X. Gao, J. Yang, J. Wu, X. Xin, Z. Li, X. Yuan, et al., "Piezoelectric Actuators and Motors: Materials, Designs, and Applications," Advanced Materials Technologies, vol. 5, no. 1, article no. 1900716, 2019.
[19] Z. Wang, B. Hou, C. Hu, and Y. Zhu, "Trajectory Compensation-Based Adaptive Control (TCAC) for High-Precision Piezoelectric Actuators," Sensors and Actuators A: Physical, vol. 375, article no. 115541, 2024.